

# PHYSICAL REVIEW LETTERS

---

---

VOLUME 77

18 NOVEMBER 1996

NUMBER 21

---

---

## Experimental Determination of the Motional Quantum State of a Trapped Atom

D. Leibfried, D. M. Meekhof, B. E. King, C. Monroe, W. M. Itano, and D. J. Wineland

*Time and Frequency Division, National Institute of Standards and Technology, Boulder, Colorado 80303-3328*

(Received 11 July 1996)

We reconstruct the density matrices and Wigner functions for various quantum states of motion of a harmonically bound  ${}^9\text{Be}^+$  ion. We apply coherent displacements of different amplitudes and phases to the input state and measure the number state populations. Using novel reconstruction schemes we independently determine both the density matrix in the number state basis and the Wigner function. These reconstructions are sensitive indicators of decoherence in the system. [S0031-9007(96)01713-9]

PACS numbers: 03.65.Bz, 32.80.Qk, 42.50.Vk

In quantum mechanics, once the density matrix of a system is determined, all knowable information is at hand. All the elusive quantum properties, like superpositions and decoherence are reflected in it. Although it is well established that the wave function or density matrix of a single quantum system cannot be determined in general, multiple measurements on an ensemble of identically prepared quantum systems can reveal their density matrix.

Early work on determination of the quantum state in such an ensemble was reviewed by Royer [1]. In quantum optics, numerous reconstruction schemes have been proposed, based on the measurement of probability distributions in different representations [2]. More recently, proposals for determining the motional state of a trapped atom have been published [3–6], partially inspired by the analogy between cavity QED and a trapped atom interacting with laser fields [7–9].

Few experiments have succeeded in determining the density matrices or Wigner functions of quantum systems. Angular momentum density matrices were measured in collisionally produced hydrogen [10], the Wigner function and density matrix of a mode of light was experimentally mapped by optical homodyne tomography [11,12], and the Wigner function of the vibrational degree of freedom of a diatomic molecule was reconstructed [13]. In this Letter we present the theory and experimental demonstration of two novel schemes that allow us to reconstruct both the density matrix in the number state basis and the Wigner function of the motional state of a single trapped

atom. A unique feature of our experiment is that we are able to prepare a variety of nonclassical input states [9] which can, for example, exhibit negative values of the Wigner function. To our knowledge these are the first experimental reconstructions revealing a negative Wigner function in position-momentum space.

In order to measure the complete state of motion, we controllably displace the input state to several different locations in phase space. Specifically, a coherent displacement [9,14]  $U(-\alpha) = U^\dagger(\alpha) = \exp(\alpha^* a - \alpha a^\dagger)$  ( $-\alpha$  is used for convenience below) is first applied to the input motional state. Here  $a$  and  $a^\dagger$  are the lowering and raising operators of the harmonically bound atom (frequency  $\omega_x$ ), while  $\alpha$  is the complex parameter characterizing the coherent amplitude and phase. We then apply radiation to the atom for a time  $t$ , which induces a resonant exchange between states  $|\downarrow\rangle|k\rangle$  and  $|\uparrow\rangle|k+1\rangle$  in a Jaynes-Cummings-type interaction [7–9]. Here  $|\downarrow\rangle$  and  $|\uparrow\rangle$  denote two selected internal states, and  $|k\rangle$  is the motional eigenstate with energy  $\hbar\omega_x(k+1/2)$ . For each  $\alpha$  and time  $t$  the population  $P_\downarrow(t, \alpha)$  of the  $|\downarrow\rangle$  level is then measured by monitoring the fluorescence produced in driving a resonant dipole cycling transition [9]. The internal state at  $t=0$  is always prepared to be  $|\downarrow\rangle$ , so the signal averaged over many measurements is [15]

$$P_\downarrow(t, \alpha) = \frac{1}{2} \left\{ 1 + \sum_{k=0}^{\infty} Q_k(\alpha) \cos(2\Omega_{k,k+1} t) e^{-\gamma_k t} \right\}, \quad (1)$$

(where  $\Omega_{k,k+1}$  are the Rabi frequencies and  $\gamma_k$  their experimentally determined decay constants). Because the Rabi frequency between  $|\downarrow\rangle|k\rangle$  and  $|\uparrow\rangle|k+1\rangle$  depends on  $k$  [9], the populations  $Q_k(\alpha)$  of the motional eigenstates after the displacement can be extracted [7–9,16]. We repeat this scheme for several magnitudes and phases of the coherent displacement and finally reconstruct the density matrix and the Wigner function from the measured displaced populations  $Q_k(\alpha)$ .

To reconstruct the density matrix  $\rho$  in the number state base, we use the relation

$$Q_k(\alpha) = \langle k|U^\dagger(\alpha)\rho U(\alpha)|k\rangle. \quad (2)$$

Note that  $Q_0(\alpha)/\pi$  is the  $Q$ -quasi-probability distribution [4]. Rewriting (2) we get

$$Q_k(\alpha) = \frac{1}{k!} \langle 0|a^k U^\dagger(\alpha)\rho U(\alpha)(a^\dagger)^k|0\rangle = \frac{1}{k!} \langle \alpha|(a-\alpha)^k \rho (a^\dagger - \alpha^*)^k |\alpha\rangle = \frac{e^{-|\alpha|^2} |\alpha|^{2k}}{k!} \sum_{n,m=0}^{\infty} \sum_{j,j'=0}^k \frac{(\alpha^*)^{n-j} \alpha^{m-j'}}{n! m!} \times (-1)^{-j-j'} \binom{k}{j} \binom{k}{j'} \sqrt{(m+j)!(n+j)!} \rho_{n+j',m+j}. \quad (3)$$

To separate the contributions of different matrix elements we may displace the state along a circle,

$$\alpha_p = |\alpha| \exp[i(\pi/N)p], \quad (4)$$

where  $p \in \{-N, \dots, N-1\}$ . The number of angles  $2N$  on that circle determines the maximum number state  $n_{\max} = N-1$  included in the reconstruction. This allows us to perform a discrete Fourier transform of Eq. (3) evaluated at the values  $\alpha_p$ , and we obtain the matrix equations

$$Q_k^{(l)} \equiv \frac{1}{2N} \sum_{p=-N}^{N-1} Q_k(\alpha_p) e^{-il(\pi/N)p} = \sum_{n=\max(0,-l)}^{\infty} \gamma_{kn}^{(l)} \rho_{n,n+l}, \quad (5)$$

with matrix elements

$$\gamma_{kn}^{(l)} = \frac{e^{-|\alpha|^2} |\alpha|^{2k}}{k!} \sum_{j'=0}^{\min(k,n)} \sum_{j=0}^{\min(k,l+n)} |\alpha|^{2(n-j-j')+l} \times (-1)^{-j-j'} \binom{k}{j} \binom{k}{j'} \frac{\sqrt{(l+n)! n!}}{(l+n-j)!(n-j)!}, \quad (6)$$

for every diagonal  $\rho_{n,n+l}$  of the density matrix. To keep the matrix dimension finite, a cutoff for the maximum  $n$  in Eq. (5) is introduced, based on the magnitude of the input state. For an unknown input state an upper bound on  $n$  may be extracted from the populations  $Q_k(\alpha)$ . If these are negligible for  $k$ 's higher than a certain  $k_{\max}$  and all displacements  $\alpha$ , they are negligible in the input state as well, and it is convenient to truncate Eq. (5) at  $n_{\max} = k_{\max}$ . The resulting matrix equation is overcomplete for some  $l$ , but the diagonals  $\rho_{n,n+l}$  can still be reconstructed by a general linear least-squares method [17].

The Wigner function for every point  $\alpha$  in the complex plane can be determined by the simple sum [16,18],

$$W(\alpha) = \frac{2}{\pi} \sum_{n=0}^{\infty} (-1)^n Q_n(\alpha). \quad (7)$$

In practice, the sum is carried out only to a finite  $n_{\max}$ , as described above. In contrast to our density matrix method

it provides a direct method to obtain the Wigner function at the point  $\alpha$  in phase space, without the need to measure at other values of  $\alpha$ . This also distinguishes the method from preceding experiments that determined the Wigner function by inversion of integral equations (tomography) [11,13].

In our experiment, the trapped atom is a single  ${}^9\text{Be}^+$  ion, stored in a rf Paul trap [19] with a pseudopotential oscillation frequency of  $\omega_x/2\pi \approx 11.2$  MHz [20]. The ion is laser cooled using sideband cooling with stimulated Raman transitions [21] between the  ${}^2S_{1/2}$  ( $F=2, m_F=-2$ ) and  ${}^2S_{1/2}$  ( $F=1, m_F=-1$ ) hyperfine ground states, which are denoted by  $|\downarrow\rangle$  and  $|\uparrow\rangle$ , respectively, and are separated by approximately 1.25 GHz.

The preparation of coherent and number (Fock) states of motion starting from the ground state is described in [9]. The coherent displacement we need for the reconstruction mapping is provided by a spatially uniform classical driving field [14,19] at the trap oscillation frequency. The rf oscillators that create and displace the state are phase locked to control their relative phase. Different displacements are realized by varying the amplitude and the phase of the displacement oscillator. For every displacement  $\alpha$ , we record  $P_l(t, \alpha)$ .  $Q_n(\alpha)$  can be found from the measured traces with a singular-value decomposition [9]. To determine the amplitude  $|\alpha|$  of each displacement, the same driving field is applied to the  $|n=0\rangle$  ground state, and the resulting collapse and revival trace is fitted to that of a coherent state [9].

The accuracy of the reconstruction is limited by the uncertainty in the applied displacements, the errors in the determination of the displaced populations, and decoherence during the measurement. The value of the Wigner function is found by a sum with simple error propagation rules. The density matrix is constructed by a linear least-squares method, and it is straightforward to calculate a covariance matrix [17]. As the size of the input state increases, decoherence and the relative accuracy of the displacements become more critical, thereby increasing their uncertainties.

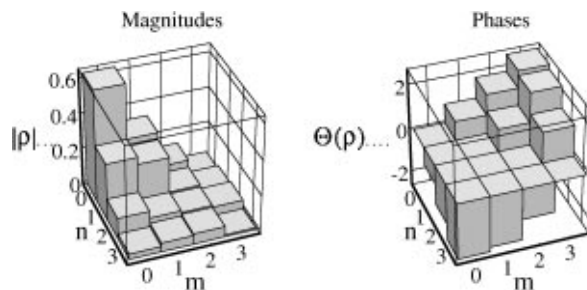
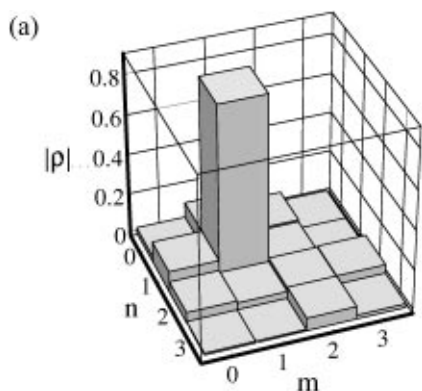


FIG. 2. Experimental amplitudes  $\rho_{nm}$  and phases  $\Theta(\rho_{nm})$  of the number-state density matrix elements of a  $|\beta| \approx 0.67$  coherent state. The state was displaced by  $|\alpha| = 0.92$ , for  $N = 4$  in Eq. (4).

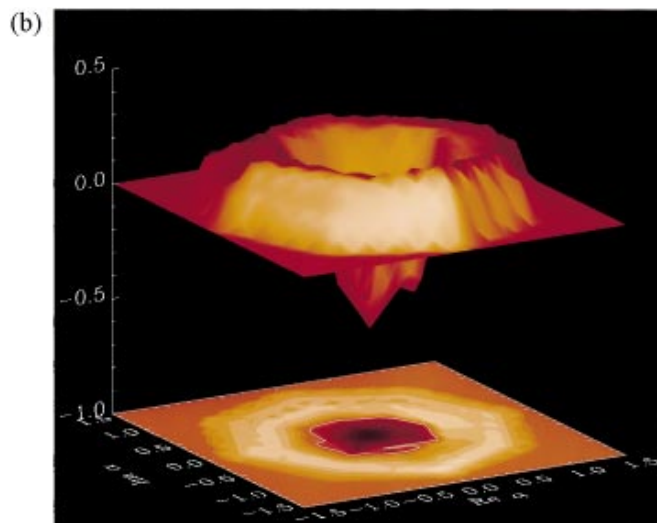


FIG. 1. (a) Reconstructed number-state density matrix amplitudes  $\rho_{nm}$  for an approximate  $|n = 1\rangle$  number state. The coherent reconstruction displacement amplitude was  $|\alpha| = 1.15(3)$ . The number of relative phases  $N = 4$  in Eq. (4), so  $n_{\max} = 3$ . (b) (color) Surface and contour plots of the Wigner function  $W(\alpha)$  of the  $|n = 1\rangle$  number state. The plotted points are the result of fitting a linear interpolation between the actual data points to a 0.1 by 0.1 grid. The octagonal shape is an artifact of the eight measured phases per radius. The white contour represents  $W(\alpha) = 0$ . The negative values around the origin highlight the nonclassical character of this state.

In Fig. 1, we show the reconstruction of both the number state density matrix (a) and Wigner function (b) of an approximate  $|n = 1\rangle$  number state. The large negative part of the Wigner function around the origin highlights the fact that the  $|n = 1\rangle$  number state is nonclassical.

In contrast, the state closest to a classical state of motion in a harmonic oscillator is a coherent state. As one example, we have excited and reconstructed a coherent state with amplitude  $|\beta| \approx 0.67$ . The experimental amplitude and phase of the number state density matrix are depicted in Fig. 2. The off-diagonal elements are generally smaller for the experiment than we would expect from the theory of a pure coherent state. In part, this is due to decoherence during the measurement, so the reconstruction shows a mixed state character rather than a pure coherent state

signature. This view is further supported by the fact that farther off-diagonal elements seem to decrease faster than direct neighbors of the diagonal. The reconstructed Wigner function of a coherent state with amplitude  $|\beta| \approx 1.5$  is shown in Fig. 3.

Next we created a coherent superposition of  $|n = 0\rangle$  and  $|n = 2\rangle$  number states. This state is ideally suited to demonstrate the sensitivity of the reconstruction to coherences. The only nonzero off-diagonal elements should be  $\rho_{02}$  and  $\rho_{20}$ , with a magnitude of  $|\rho_{02}| = |\rho_{20}| = \sqrt{\rho_{00}\rho_{22}} \approx 0.5$  for a superposition with about equal probability of being measured in the  $|n = 0\rangle$  or  $|n = 2\rangle$  state. In the reconstruction shown in Fig. 4 the populations  $\rho_{00}$  and  $\rho_{22}$  are somewhat smaller, due to imperfections in the

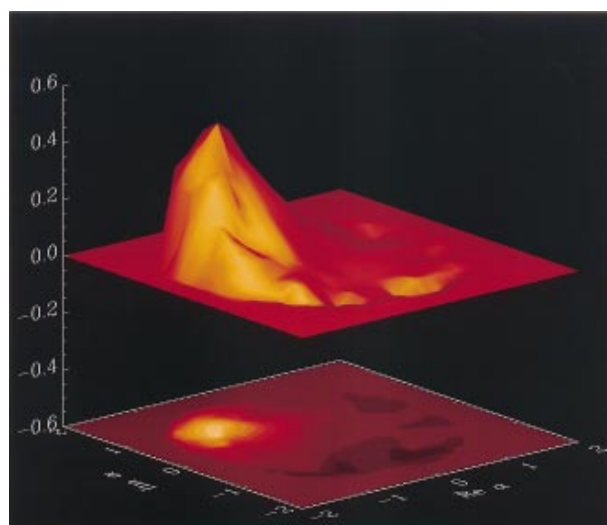


FIG. 3(color). Surface and contour plots of the reconstructed Wigner function of a coherent state. The plotted points are the result of fitting a linear interpolation between the actual data points to a 0.13 by 0.13 grid. The approximately Gaussian minimum uncertainty wave packet is centered around a coherent amplitude of about 1.5 from the origin. The half width at half maximum is about 0.6, in accordance with the minimum uncertainty half width of  $\sqrt{(1/2)\ln(2)} \approx 0.59$ . To suppress artifacts in the Wigner function summation, we have averaged over  $n_{\max} = 5$  and  $n_{\max} = 6$  truncations, as suggested by M. Collett.

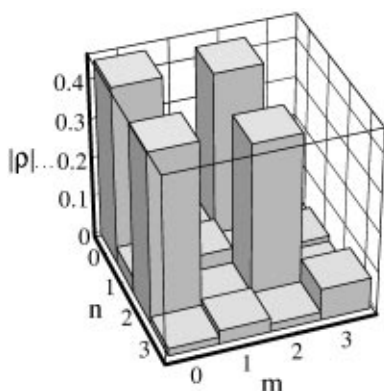


FIG. 4. Reconstructed density matrix amplitudes of an approximate  $1/\sqrt{2}(|n=0\rangle - i|n=2\rangle)$  state. The state was displaced by  $|\alpha| = 0.79$  for  $N = 4$  in Eq. (4). The amplitudes of the coherences indicate that the reconstructed density matrix is close to that of a pure state.

preparation, but the coherence has the expected value of  $|\rho_{20}| = |\rho_{02}| \approx \sqrt{\rho_{00}\rho_{22}}$ .

In contrast to the above, a thermal state should exhibit no coherences. In the experiment such a state was prepared by (only) Doppler cooling the ion [9]. The reconstruction of the resulting thermal state with mean occupation number  $\bar{n} \approx 1.3$  is depicted in Fig. 5. As expected, there are no coherences, and the diagonal, which gives the number state occupation, shows an exponential behavior within the experimental errors.

In summary, we have created number, thermal, coherent, and number-state superposition states of motion of a trapped atom and determined both density matrices in the number-state basis and Wigner functions of these states. The methods are suitable for arbitrary quantum states of motion, including mesoscopic superposition states (Schrödinger's cat states) [22] and could be a useful tool to study decoherence in these states. These methods could also be implemented in cavity-QED experiments to deter-

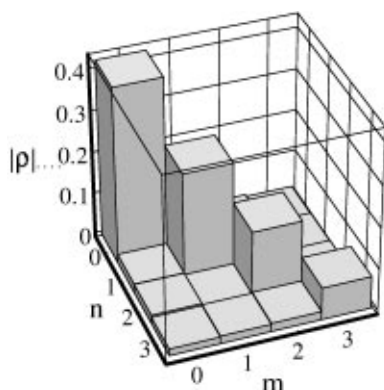


FIG. 5. Reconstructed density matrix of a  $\bar{n} \approx 1.3$  thermal state. This state was displaced by  $|\alpha| = 0.78$ , for  $N = 4$  in Eq. (4). As one would expect for a thermal state, no coherences are present within the experimental uncertainties and the populations drop exponentially for higher  $n$ .

mine the states of an electromagnetic field (using available techniques) [23], or in neutral atom traps where dipole forces could provide the drive for a coherent displacement [9,22]. Another straightforward extension of this work in ion traps would be to perform tomography on entangled motional and internal states of two or more trapped ions, by combining the motional state reconstruction with Ramsey-type and correlation experiments.

This work is supported by the U.S. National Security Agency, the Office of Naval Research, and the Army Research Office. D.L. acknowledges a Deutsche Forschungsgemeinschaft research grant. D.M.M. is supported by a N.R.C. postdoctoral fellowship. We thank W. Vogel for pointing out the connection of the Wigner function to the displaced populations and J.I. Cirac and P. Zoller for stimulating discussions. We acknowledge important contributions by J. Bergquist and helpful comments on the manuscript by M. Young, J.J. Bollinger, P. Huang, and M. Holland.

*Note added.*—After submission of this work we have learned that Mlynek *et al.* have measured the Wigner function of atoms in an interferometer [24], and that Opatrny *et al.* [25] propose a very similar method to reconstruct the density matrix of a light field in the number-state basis.

- 
- [1] A. Royer, *Found. Phys.* **19**, 3 (1989).
  - [2] K. Vogel and H. Risken, *Phys. Rev. A* **40**, 2847 (1989).
  - [3] S. Wallentowitz and W. Vogel, *Phys. Rev. Lett.* **75**, 2932 (1995).
  - [4] J.F. Poyatos, R. Walser, J.I. Cirac, P. Zoller, and R. Blatt, *Phys. Rev. A* **53**, R1966 (1996).
  - [5] C. D'Helon and G.J. Milburn, *Phys. Rev. A* **54**, R25 (1996).
  - [6] P.J. Bardorff, C. Leichtle, G. Schrade, and W.P. Schleich (to be published).
  - [7] C.A. Blockley, D.F. Walls, and H. Risken, *Europhys. Lett.* **77**, 509 (1992).
  - [8] J.I. Cirac, R. Blatt, A.S. Parkins, and P. Zoller, *Phys. Rev. A* **49**, 1202 (1994).
  - [9] D.M. Meekhof, C. Monroe, B.E. King, W.M. Itano, and D.J. Wineland, *Phys. Rev. Lett.* **76**, 1796 (1996).
  - [10] J.R. Ashburn, R.A. Cline, P.J.M. van der Burgt, W.B. Westerveldt, and J.S. Risley, *Phys. Rev. A* **41**, 2407 (1990).
  - [11] D.T. Smithey, M. Beck, M.G. Raymer, and A. Faridani, *Phys. Rev. Lett.* **70**, 1244 (1993).
  - [12] G. Breitenbach, T. Müller, S.F. Pereira, J.Ph. Poizat, S. Schiller, and J. Mlynek, *J. Opt. Soc. B* **12**, 2304 (1995).
  - [13] T.J. Dunn, I.A. Walmsley, and S. Mukamel, *Phys. Rev. Lett.* **74**, 884 (1995).
  - [14] P. Carruthers and M.M. Nieto, *Am. J. Phys.* **7**, 537 (1965).
  - [15] Equation (2) of Ref. [9] is in error and should be replaced by Eq. (1) here.
  - [16] In this experiment we can consider the internal atomic state to be the detector. If we neglect noise and decoherence in the mapping operations, the motional state information is mapped according to Eq. (1) with unit

- efficiency onto the  $|\downarrow\rangle$  state. Therefore, to have unit detection efficiency in the experiment, it is not necessary to detect the  $|\downarrow\rangle$  state with unit efficiency. The analogy with photon detection would be a 100% efficient detector which is read out only sporadically.
- [17] W.H. Press, S.A. Teukolsky, W.T. Vetterling, and B.P. Flannery, *Numerical Recipes* (Cambridge University Press, Cambridge, 1986), Chap. 14.3.
- [18] A. Royer, Phys. Rev. Lett. **52**, 1064 (1984); H. Moya-Cessa and P.L. Knight, Phys. Rev. A **48**, 2479 (1993); S. Wallentowitz and W. Vogel, Phys. Rev. A **53**, 4528 (1996); K. Banaszek and K. Wodkiewicz, Phys. Rev. Lett. **76**, 4344 (1996).
- [19] S. Jefferts, C. Monroe, E. Bell, and D.J. Wineland, Phys. Rev. A **51**, 3112 (1995).
- [20] For the parameters of this experiment, the effects of rf “micromotion” are small and can be neglected. A thorough treatment which includes the micromotion is described in Ref. [6].
- [21] C. Monroe, D.M. Meekhof, B.E. King, S.R. Jefferts, W.M. Itano, D.J. Wineland, and P.L. Gould, Phys. Rev. Lett. **75**, 4011 (1995).
- [22] C. Monroe, D.M. Meekhof, B.E. King, and D.J. Wineland, Science **272**, 1131 (1996).
- [23] M. Brune, F. Schmidt-Kaler, A. Maali, J. Dreyer, E. Hagley, J.M. Raymond, and S. Haroche, Phys. Rev. Lett. **76**, 1800 (1996).
- [24] J. Mlynek (private communication).
- [25] T. Opatrny and D.-G. Welsch (to be published).